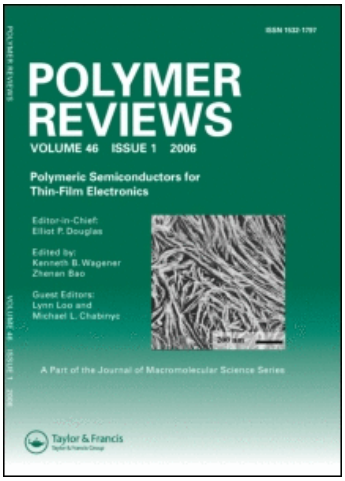

Polymer Reviews
Publication details, including instructions for authors and subscription information:
http://www.informaworld.com/smpp/title~content=t713597276

SANS from Polymers—Review of the Recent Literature

Boualem Hammouda [a]
[a] National Institute for Standards and Technology, Center for Neutron Research, Gaithersburg, MD

Online publication date: 22 February 2010

To cite this Article Hammouda, Boualem(2010) 'SANS from Polymers—Review of the Recent Literature', Polymer Reviews, 50: 1, 14 — 39
To link to this Article: DOI: 10.1080/15583720903503460
URL: http://dx.doi.org/10.1080/15583720903503460

Journal of Macromolecular Science®, Part C: Polymer Reviews, 50:14–39, 2010

ISSN: 1558-3724 print / 1558-3716 online
DOI: 10.1080/15583720903503460

Reviews

SANS from Polymers—Review of the Recent Literature

BOUALEM HAMMOUDA

National Institute for Standards and Technology, Center for Neutron Research, Gaithersburg, MD

This paper reviews the recently published literature on Small-Angle Neutron Scattering (SANS) from polymers. Papers published over the past three years and resulting from the use of the NIST Center for Neutron Research (NCNR) are included. Those with which this author is most familiar are summarized in a brief format. The intent of this review paper is to demonstrate the usefulness of the SANS technique and its impact on polymer research. SANS is a structural characterization method and a good probe for miscibility thermodynamics in polymer mixtures. SANS topics covered include polymer solutions, copolymers, polymer blends, branched or grafted polymers, polymer gels, polymer networks, polymer micelles, polymeric nanomaterials, and polymer membranes.

Keywords small range neutron scattering, polymer structures, nanoscale, polymer solutions, copolymers, blends, gels, networks, branched polymers

1. The SANS Technique

Small-angle neutron scattering (SANS) is an effective characterization method to investigate nanoscale structures. It is based at neutron scattering facilities and has experienced steady growth over the past thirty years. It probes structures with sizes from the near atomic to the near micrometer scale and has had impact in many research areas including polymers, complex fluids, biology, and materials science. The partial deuteration method (which consists of replacing hydrogen by deuterium atoms) gives the SANS technique unique advantage. Like other scattering methods, SANS yields measurements in the reciprocal (Fourier transform) space and depends therefore on data interpretation using models and not on direct space imaging like microscopy.

The SANS instrument uses the following basic steps:

1. monochromation, 2. collimation, 3. scattering and 4. detection (Fig. 1).

Monochromation consists of producing a monochromatic neutron beam from the Maxwellian neutron source spectrum and is performed using a velocity selector. Collimation is performed using a source aperture and a sample aperture in order to define an

Received June 18, 2009; accepted October 27, 2009.
Address correspondence to Dr Boualem Hammouda, Center for Neutron Research, 100 Bureau Drive, Gaithersburg 20899-6102, United States. E-mail: hammouda@nist.gov

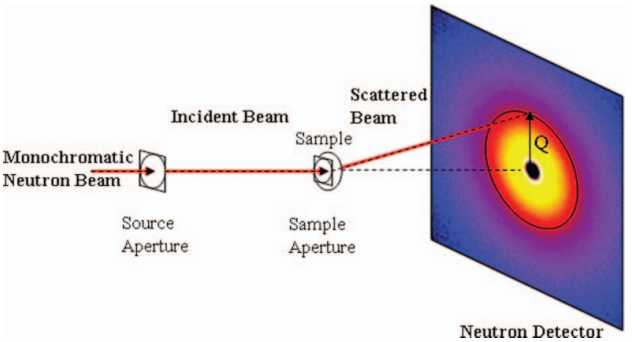

Figure 1. Schematics of a SANS instrument. This Figure is not to scale; the total horizontal size is 30 m whereas the neutron detector height is 64 cm.

incident neutron beam with very small divergence. Scattering from samples of various forms (liquids, solids, gels, etc.) and in various environments (heating, pressure, shear, applied magnetic field, etc.) is measured in special cells. Detection of the scattered neutrons is performed using a 2D area sensitive detector. The pre-sample and the post-sample flight paths can be adjusted between 1 m and 15 m distance. The overall size of a SANS instrument is typically 30 m. The sample thickness is between 1 mm and 2 mm making the SANS technique a bulk probe.

The NIST Center for Neutron Research (NCNR) facility operates two 30 m SANS instruments at the core of a thriving user program. Research on SANS from polymers constitutes the most active component.

2. SANS Data Analysis and Modeling

Various aspects of the SANS technique including data analysis methods can be found in a recent book available online.[1] SANS data analysis consists of one of three methods.

1. Rapid interpretation using standard (linear) plots such as the Guinier plot (to obtain a radius of gyration) or the Porod plot (to obtain a Porod exponent). Porod exponents vary between 1 (for 1D object such as a rod) and 4 (object with smooth surface). For example, the Porod exponent of a polymer coil in a good solvent is 5/3 while that for a polymer coil in poor solvent is 3. A Porod exponent of 2 characterizes either a polymer coil in theta solvent or a 2D structure (such as a lamella). This first data analysis method is used routinely. Extensive description of linear plots can be found in Chapter 22 of the SANS Toolbox.[1]
2. Nonlinear least-squares fitting to appropriate models. A large number of models are available for the analysis of SANS data from polymer systems. These are either for macromolecular scattering such as the Random Phase Approximation (RPA) or for particulate scattering such as the analytical solutions of the Ornstein-Zernike (OZ) equation. Polymer solutions and homogeneously mixed blends are well described by the RPA model while the various microphases in block copolymers (spherical, cylindrical, lamellar, etc.) are best described by solutions to the OZ equation. One such solution, the Percus-Yevick equation, offers a simple analytical form for hard-sphere interaction potential between spherical particles. The Mean Spherical Approximation is another analytical solution of the OZ equation for charged particulate systems. The zero average contrast method consists of using deuterated and non-deuterated polymer mixtures as well as deuterated and nondeuterated solvent

mixtures in order to isolate the single-chain form factor even from concentrated polymer solutions. This method has been applied to polymer blend mixtures as well. Smearing of the models to account for instrumental resolution is performed prior to the fitting step. This second data analysis method is the most used. The RPA, the zero average contrast method, and the OZ models are described in detail in Chapters 31 and 32 of the SANS Toolbox respectively.[1]

3. Particle shape reconstruction and inverse Fourier transform methods are sophisticated approaches that perform in-depth analysis of SANS data using canned software packages. This data analysis method is rarely used owing to its high level of specificity.

The SANS signal is characterized by a constant (Q-independent) part due to incoherent scattering from (mostly) hydrogen in the sample as well as by a Q-dependent coherent scattering part which contains information about structure, morphology and phase transitions in the sample. Here Q is the scattering variable given in terms of the neutron wavelength λ and scattering angle θ as $Q = (4\pi/\lambda)\sin(\theta/2)$. The coherent scattering cross section (units of cm^{-1}) can be expressed as:

$$\frac{d\Sigma(Q)}{d\Omega} = \phi \Delta\rho^2 V_P P(Q) S_I(Q). \quad (1)$$

Here ϕ is the volume fraction and V_P is the volume of the scattering "objects," $\Delta\rho^2$ is the neutron contrast factor, P(Q) is the single object form factor, and $S_I(Q)$ is the inter-object structure factor. The scattering objects can be either polymer coils for macromolecular scattering or compact "particles" in the case of particulate scattering. The SANS Toolbox[1] contains the form factors for various shape objects (Chapter 27) as well as for polymer chains with excluded volume (Chapter 28).

The SANS technique is sensitive to composition fluctuations and is therefore a good probe for phase transition studies in polymer mixtures. The thermodynamics of miscibility are well described by the RPA model which predicts (for instance) the spinodal phase transition condition. Polymer mixtures (solutions or blends) either phase separate upon heating and are characterized by a lower critical solution temperature (LCST) or upon cooling and are characterized by an upper critical solution temperature (UCST). The mean field RPA approach uses the Flory-Huggins interaction parameters which can be measured by SANS.

3. SANS from Polymers

A large number of SANS research from polymers has been covered at the tutorial level in the SANS Toolbox[1] which contains a great deal of topics borrowed from this author's research efforts. Chapter 37 describes the use of an empirical model to extract the correlation length (average distance between entanglements) in a semidilute polymer solution, applies the zero average contrast method to extract single-chain properties such as the radius of gyration and uses a simple extrapolation method to obtain an estimate of the spinodal (phase separation) temperature for an LCST system. Chapter 38 uses the Flory-Huggins Gibbs free energy to map out the phase diagram for a model polyolefin blend. Flory-Huggins interaction parameters were estimated and found to depend inversely on (absolute) temperature. The binodal and spinodal temperatures and the nucleation-and-growth region in-between were plotted. Chapter 39 describes SANS from copolymers. Here also, the RPA method is used to predict the order-to-disorder line for a diblock copolymer. SANS from copolymer spectra

are characterized by a peak due to the correlation hole effect in the homogeneous phase or due to inter-domain spacing in the ordered phases. Ordered phases correspond to spherical, cylindrical, and lamellar morphologies (mostly). Chapter 40 summarizes SANS results from a ternary blend mixture in which two of the homopolymers are hydrogenated (i.e., non-deuterated). The Flory-Huggins interaction parameters were extracted for all three polymer pairs including the hydrogenated pair.

Chapter 43 makes use of a sophisticated model to interpret SANS data from a crystalline polymer in solution. Thicknesses of the amorphous and lamellar regions as well as the number of lamellae per stack were obtained. A material balance approach was used along with nonlinear least squares fits to this model. Chapter 44 describes micelle formation in a triblock (Pluronic) copolymer solution. The unimers-to-spherical micelles conditions (temperature and concentration) were estimated. Cylindrical and lamellar micelles were also obtained upon further heating.

The use of judicious sample environments has contributed greatly to the SANS from polymers research effort. Chapter 52 and 53 illustrate some of this effort using in-situ pressure and shear respectively. Use of the compressible RPA model along with an equation-of-state yielded an estimation of the amount of free volume present in polymer blends. The use of the Clausius-Clapeyron equation helped predict the effect of pressure on the spinodal line. In some systems, pressure favored mixing while in other cases, it favored demixing. In-situ shear produces appealing 2D spectra with lots of spots and anisotropic features. Pluronic spherical micelles formed body-centered cubic structures that changed into face-centered cubic structures under Couette shear. Twinned structures were also observed.

This review paper references some 76 papers on SANS from polymers resulting from use of the NCNR over the past three years. They are cataloged into broad categories that include polymer solutions,[2–9] copolymers,[10–19] polymer blends,[20–23] branched or grafted polymers,[24–32] polymer gels,[33–40] polymer networks,[41–48] polymer micelles,[49–63] polymeric nanomaterials,[64–70] and polymer membranes.[71–77] Of these papers, about half are briefly summarized in order to represent the breadth of ongoing research. Those summarized are the ones with which this author is the most familiar with.

4. Polymer Solutions

Chain conformations and demixing phase behaviors are common topics investigated using SANS from polymer solutions. Such topics include characteristic chain dimensions for various stiff or flexible polymers, polymer-solvent interactions, and phase transitions. Investigations of solution crystallization have been included in this section.

Poly(cyclohexdiene) (PCHD) polymers contain six-member rings on the main chain. This characteristic gives them much desired mechanical properties and good thermal stability when compared to other vinyl polymers. For instance, PCHD polymers have the highest glass-rubber transition temperature (T_g around 231°C) of all hydrocarbon polymers. Solution properties of PCHD polymers in tetrahydrofuran and in chloroform solutions were investigated using conventional methods that included light scattering and SANS.[2] These two techniques measured the radius of gyration (R_g) and the second virial coefficient (A_2) as a function of polymer concentration, temperature, and solvent quality. The Zimm plot method was used; it consists of an extrapolation to low scattering variables (Q) and low polymer fractions. A simple wormlike chain model reproduced the measured radii of gyration. It was found that the PCHD chain conformations were stiffer in chloroform than in tetrahydrofuran solutions.

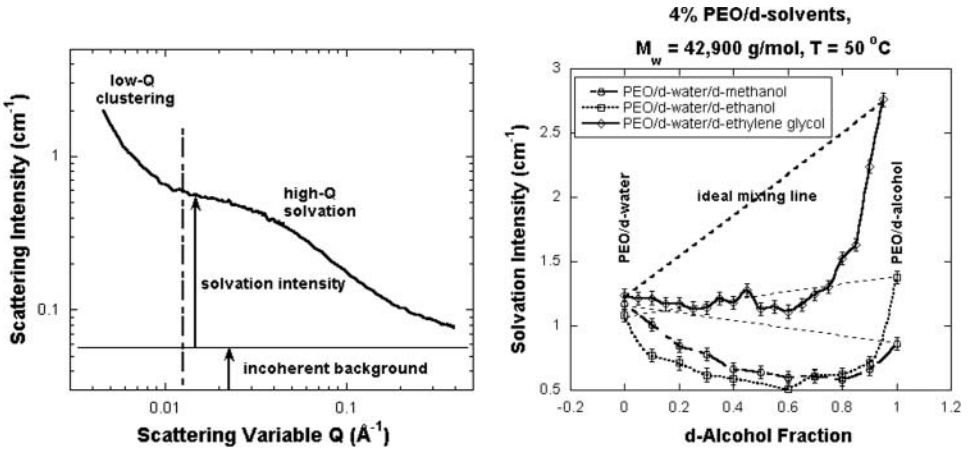

Figure 2. SANS spectrum from 4% poly(ethylene oxide) mass fraction in d-water (left) showing the high-Q coherent signal (solvation intensity) and the constant incoherent background. The solvation intensity is plotted for 4% PEO in d-water/d-alcohol solvent mixtures (right). Non-ideal mixing is observed in all cases. The error bars correspond to one standard deviation.

The model water-soluble polymer poly(ethylene oxide) $[–CH_2CH_2O–]_n$ was used to investigate solvation properties in binary solvent mixtures consisting of water and other solvents (methanol, ethanol, ethylene glycol). The SANS technique was used to obtain a wide Q range.[3] Deuterated solvents were used in order to enhance the neutron contrast. At low-Q, large length-scale features are characteristic of clustering (PEO in d-water) or crystallization (PEO in alcohols). The high-Q region probes polymer-solvent interactions (the solvation layer) as well as their mixing behavior (Fig. 2). The measurement temperature was kept above the crystal melting temperature when crystallization was present. A simple empirical model was used to fit SANS data and obtain solvation intensity, a correlation length, and a Porod exponent. The correlation length is an estimate of the average entanglement distance in the semidilute PEO solutions. Moreover, the random phase approximation model was used to back out Flory-Huggins interaction parameters for the ternary mixture PEO/d-water/d-methanol. It was found, for instance, that the solvation intensity for PEO in binary solvent mixtures was always lower than the ideal mixing prediction; non-ideal mixing seems to be the norm for PEO in mixed solvents. Mixed solvents seem to be better solvating agents for PEO than the individual solvents.

The SANS technique was also used to investigate the solvation behavior of PEO in d-water in the dilute and semidilute regimes.[4] The correlation length (obtained from the empirical model) was seen to decrease in dilute solutions but to increase in semidilute solutions. This behavior change yields an accurate method for measuring the overlap concentration used to delimit dilute from semilute solutions. The decrease in coil size in the dilute region is the precursor to the single-coil collapse transition that occurs in extremely dilute solutions of polymers with extremely high molecular weights. The temperature dependence of the correlation length shows that its inverse follows a linear behavior when plotted versus 1/T (where T is the absolute sample temperature). It remains to be seen whether this "universal" behavior observed for PEO would hold for other polymers in solution.

Poly(ethylene oxide) assumes a coil conformation when dissolved in water, but it assumes a helical conformation when dissolved in isobutyric acid along with trace amounts

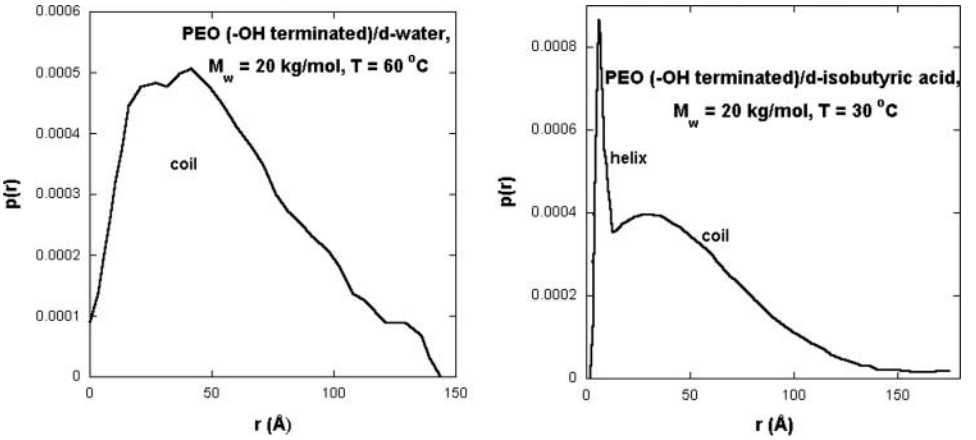

Figure 3. Pair distribution function for a poly(ethylene oxide) solution in d-water (left) and in d-isobutyric acid (right). This distribution was obtained through the Fourier transform of the SANS data. The distribution on the right is characteristic of a mixture of helix and coil phases.

of water. The helix-to-coil transition can be reversibly effected by adding/removing trace amounts of water. SANS and polarimetry measurements were used to investigate the helical and coil structures in various solvent and temperature conditions.[5] A number of data analysis methods and software packages were used to analyze the SANS data. These included standard plots (such as the Porod plot), fits to cylindrical structure models (to represent the helical structure), and inverse Fourier transform of the data to obtain a pair distribution function p(r). Porod exponents close to 1 were observed for rod-like (helical) structures at low-Q and close to 5/3 for swollen polymer coils. Note that the helical structures are characterized by high-Q Porod exponents close to 4 (smooth rod surfaces). The pair distribution functions showed pure coil phases for PEO/d-water and helical phases in PEO/d-isobutyric acid (Fig. 3). Mixtures of coil and helical phases were observed for high molecular weight PEO/d-isobutyric acid. The helical structure in solution was reminiscent of the crystalline structure of pure PEO (whereby 7 monomeric units form 2 helical turns). Similar investigations were performed on another (similar) water-soluble polymer, poly(ethylene imine), referred to as PEI $[–CH_2CH_2NH–]_n$ both in d-water and in d-isobutyric acid and similar conclusions were obtained. The helical structures were better developed with PEI than with PEO.

The partitioning of PEO in water/isobutyric acid solvent mixtures was further investigated using SANS. Low molecular weight polymers (with $M_w < 10$ kg/mol) were seen to prefer dissolving in the isobutyric acid rich (top) phase and higher molecular weight ones end up mostly in the water (bottom) phase. Investigations of the phase boundaries for the PEO/water/ isobutyric acid ternary mixture were conducted.[6] It was found that the addition of PEO tends to favor demixing in water/isobutyric acid solvent mixtures. Similar conclusions were obtained using star branched PEO instead of linear PEO.

The early stages of crystallization of (low-molecular weight) polyethylene in d-xylene solutions were investigated by SANS.[8] Crystallization was obtained upon cooling from the melt state (at 120°C) down to temperatures varying from 110°C to 85°C. Very early stages of crystal growth were investigated. The SANS technique was found to be sensitive to crystal volume fractions as small as 10^{-5}. This sensitivity is much better than for SAXS where

low-Q background interferes with the useful signal. SAXS is the main diagnostic tool for investigations of polymer crystallization. Two competing modes of early-stage crystallization were presented with either spinodal decomposition or nucleation-and-growth as the driving force. The high sensitivity SANS measurements reported here favor the nucleation-and-growth (crystal seeding-and-growth would be a better name) mechanism. Investigations of the late-stage crystal growth with well-formed lamellae were also discussed.

Poly(ethylene oxide) forms a crystalline structure when dissolved in ethanol. SANS investigations were conducted on dilute and semidilute solutions of PEO/d-ethanol for temperatures above and below the crystallization temperature.[9] Above the crystal melting temperature, fully-swollen polymer coils were observed while below the crystallization temperature, a sponge-like lamellar morphology was reported. DSC, WAXS, and confocal microscopy confirmed the SANS findings. The PEO/d-ethanol phase diagram showing both the crystallization and the extrapolated spinodal line has been mapped out. The extrapolated upper critical solution temperature (UCST) was found to be well below the crystallization temperature and therefore unreachable. The addition of a small amount of d-water to the PEO/d-ethanol mixture was found to destroy the crystalline morphology and yield regular polymer solution behavior. The phase diagram was seen to change to a lower critical solution temperature (LCST) when the water amount is increased.

5. Copolymers

There are three categories of SANS investigations from copolymers; these used pure copolymers, copolymers in solution, and copolymers added to blends. These categories are represented here.

The conformation of polymer chains in regular symmetric multiblock copolymers was investigated using SANS measurements from previously sheared samples.[10] Symmetric copolymers tend to form lamellar structures which, when sheared, tend to align according to the "parallel" or A alignment (lamellae oriented in the shear/shear gradient plane) or the "perpendicular" C alignment (lamellae orientated in the shear/vorticity plane). The B alignment (lamellae oriented in the shear gradient/vorticity plane) is never observed under shear; it is observed only after shear cessation. The undecablock (containing 10 blocks) of poly(cyclohexylethylene) and poly(ethylene propylene) was used for these investigations. Mixtures of undecablocks and deuterated undecablocks (in equal fractions) were prepared in order to separate out scattering from the multiblock structure (characterized by an interblock Bragg peak) and scattering from partially deuterated polymer chain conformations (characterized by the radius of gyration for the entire copolymer). The Guinier plot at low scattering variable Q was used to measure this radius of gyration. These investigations showed that polymer chains tend to align in the B alignment plane when lamellae are aligned along the C alignment plane. Shear cessation relaxes the stretched copolymers into a 3D random walk spread out over many lamellar microdomains.

The SANS technique was used to investigate vesicle formation when a poly(ethylene oxide)-poly(butylene oxide) diblock copolymer (EO_6BO_{11}) is dissolved in water.[12] The hydrophobic nature of the BO block drives the vesicle formation. At low diblock fraction and temperature, a wormlike micelle phase is observed. This is characterized by a 1/Q Porod behavior at low-Q (cylindrical structures). As the diblock fraction or temperature is increased, unilamellar, then multilamellar vesicles form. These are characterized by a $1/Q^2$ Porod behavior at low-Q (2D structures) and a Bragg peak at high-Q. At even higher diblock fraction or temperature, the vesicles form a lamellar phase. Indirect Fourier transform of the SANS data produced pair correlation functions which yielded estimates of vesicle sizes.

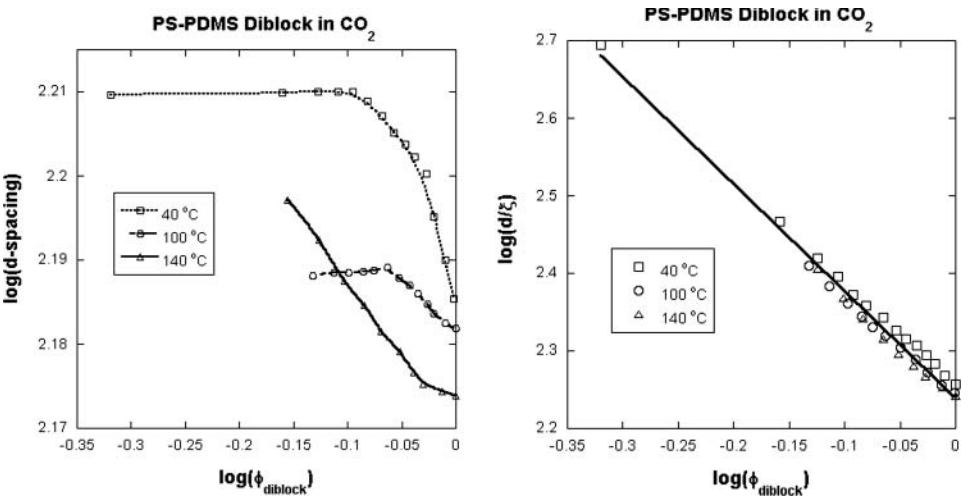

Figure 4. Variation of the d-spacing (left) and of its ratio to the swelling asymmetry factor d/ξ for the PS-PDMS diblock copolymer in CO_2.

A morphology phase diagram (temperature versus diblock copolymer fraction in d-water) was mapped out.

Pressurized CO_2 plays the role of a selective solvent in a polystyrene-poly(dimethyl siloxane) diblock copolymer.[16] This PS-PDMS copolymer is characterized by lamellar morphology with well-defined interdomain d-spacing. This d-spacing is inversely proportional to the scattering peak position. The SANS technique is useful for the characterization of this d-spacing as well as estimation of the various Flory-Huggins interaction parameters between each of the blocks (PS or PDMS) and the solvent (CO_2) and between the two blocks (PS-PDMS). The swelling conditions are described by swollen block volume fractions f_{PS/CO_2} and f_{PDMS/CO_2}. These are determined from an equation-of-state for the swelling of the pure components (PS and PDMS) in CO_2 along with the Flory-Huggins equation for polymer/solvent mixtures. Their ratio defines a swelling asymmetry factor $\xi = f_{PS/CO_2}/f_{PDMS/CO_2}$. SANS data were taken from the PS-PDMS diblock copolymer under CO_2 pressure for three temperatures (40°C, 100°C, and 140°C). It was noted that whereas the interlamellar d-spacing (noted d) varies with the copolymer volume fraction ϕ_{diblock} differently for each temperature, the ration d/ξ follows the same power law for all temperatures (Fig. 4).

The microphase behavior for a series of poly(styrene sulfonate)-poly(methyl butylene) diblock copolymers was investigated using the SAXS and SANS techniques.[17] High resolution of the SAXS technique allows the indexing of numerous Bragg reflections and therefore the possibility of resolving a wide range of ordered diblock copolymer microstructures. The observed copolymer morphologies include lamellae, gyroid, hexagonally perforated lamellae, and hexagonally packed cylinders. These morphologies were obtained by varying the copolymer molecular weight and sulfonation level as well as temperature. This range of morphologies was obtained with nearly symmetric diblock copolymers. TEM images confirmed some of the observed morphologies. SANS data were taken to estimate the Flory-Huggins interaction parameter which was used to predict the order-disorder transition conditions.

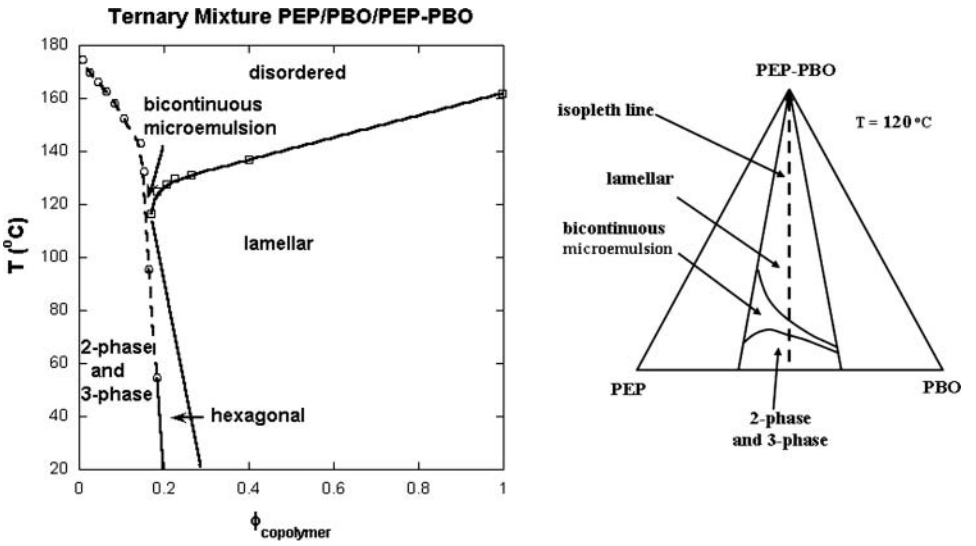

Figure 5. Phase diagram for the PEP/PBO/PEP-PBO ternary mixture for increasing copolymer fraction (left); i.e., along the isopleth line which is depicted within the triangle phase diagram (right).

The ternary phase diagram for a polymer mixture consisting of two homopolymers, poly(ethylene propylene) and poly(butylene oxide), and their diblock copolymer PEP-PBO has been investigated using a host of characterization methods that include SANS, small-angle x-ray scattering (SAXS), rheology, and optical microscopy.[18] Deuterated PEP was used in order to enhance the SANS contrast. A ternary phase diagram similar to the one for a nonionic surfactant/water/oil micellar system was mapped out close to the isopleth line (line for equal homopolymer fractions but with increasing copolymer fraction). The upper critical binodal line for the PEP/PBO binary blend was also mapped out. Along the isopleth line, the phase separation boundaries between the mixed phase, the macrophase separated region, and the microphase separated region were delimited. Within the microphase separation region, the order-to-order phase transition lines for the lamellar and hexagonal microphases were obtained (note that no cubic phase was observed). SAXS was effective at differentiating the ordered phases. The macrophase separation region contains two-phase droplets (rich in PEP or PBO with PEP-PBO forming the boundary between them) and three-phase droplets (rich in PEP, in PBO, or in PEP-PBO). The SANS technique was useful for the characterization of a narrow bicontinuous microemulsion channel obtained for high copolymer fraction (80%) and high temperature (around 120°C). The Teubner-Strey model was used to fit the SANS data (Fig. 5).

A-C diblock copolymers were mixed to weakly-segregated A/B homopolymer blends. Components A, B, and C used were polybutadiene (89% 1,2 addition), polyisobutylene and polybutadiene (63% 1,2 addition) respectively.[19] The C block was characterized by attractive interactions with the B block but repulsive interactions with the A block. This SANS study showed that organized domains form with the addition of as little as 1% A-C diblock to a 50%/50% A/B blend. SANS data were taken from a series of samples for which the copolymer fraction as well as its molecular weight were varied. The random phase approximation (RPA) model was used to analyze SANS data in the homogeneous (mixed) phase region. The Teubner-Strey (TS) model and a self-consistent-field theory

(SCFT) were used in the ordered microphase region. The RPA approach yielded Flory-Huggins interaction parameters and mean-field phase boundary predictions. The TS model and the SCFT approach yielded predictions of characteristic microdomain d-spacings as observed by SANS. The combination of measurements and models produced reasonable agreement for most of the probed range except for the case with very small copolymer fractions where there is room for improvement.

6. Polymer Blends

Polymer blends constitute another active area of SANS research. The SANS technique is sensitive to density and composition fluctuations and is therefore a good thermodynamic probe for investigation of phase transitions in blends.

The same polymer blend A/B/A-C discussed before[19] was used to investigate the effects of pressure on phase transitions.[20] Block C is characterized by repulsive interactions with block A and attractive interactions with block B. At ambient pressure, the blend forms a lamellar microphase at low temperature, a bicontinuous microemulsion phase at intermediate temperature, and is macrophase separated at high temperature. The same blend, however, exhibits a mixed (homogeneous) phase when pressurized. This behavior was traced to intricate dependences of the Flory-Huggins interaction parameters on temperature and pressure; χ_{AC} (positive) decreased with temperature but did not change with pressure, χ_{BC} (negative) increased with temperature but decreased (became more negative) with pressure, and χ_{AB} (positive) increased with temperature but decreased with pressure. The random phase approximation (RPA) and the self-consistent-field theory (SCFT) were used to analyze SANS data with in-situ pressure. The Teubner-Strey model was also used to fit data in the microemulsion phase region. A pressure-temperature phase diagram was mapped out showing boundaries between the microphase separation, the macrophase separation, and the homogeneous mixed-phase regions (Fig. 6). The observation that pressure induces the formation of a homogeneous phase (favoring mixing) in the A/B/A-C polymer blend is contrary to the observed effect of pressure in nonionic surfactant/water/oil ternary mixtures where pressure tends to favor demixing.

The SANS technique can map out both the binodal line and the spinodal line. The binodal line is reached when the intercept of the Zimm plot $I^{-1}(0)$ becomes negative (here I(0) is the scattering intensity in the forward $Q = 0$ direction). The spinodal line is obtained by extrapolating the $I^{-1}(0)$ versus T^{-1} linear behavior to the limit $I^{-1}(0) = 0$ (here T is the absolute sample temperature). This helps delimit the nucleation-and-growth region located between the binodal and spinodal lines. Growth kinetics were studied by SANS from a deuterated poly(methylbutylene)/poly(ethylbutylene) off-critical polyolefin blend sample following pressure jumps from the homogeneous (mixed) phase region into the nucleation-and-growth region.[21] Pressure jumps are more rapid than temperature jumps and therefore more effective. Prior to jump experiments, the pressure-temperature phase diagram (showing both the binodal and spinodal lines) was mapped out for the same dPMB/PEB blend. Nucleation-and-growth kinetics measurements were performed for a number of pressure jumps and for many quench depths. Both single jumps and double jumps were performed. In the case of double jumps, the first jump was deep into the nucleation-and-growth region (to form the nucleation seeds) and the second jump was shallow (to follow the growth kinetics). Critical nucleus sizes and the times required to conclude the early stage of nucleation were measured. These were obtained from the time-dependent SANS intensity characterizing the growth kinetics.

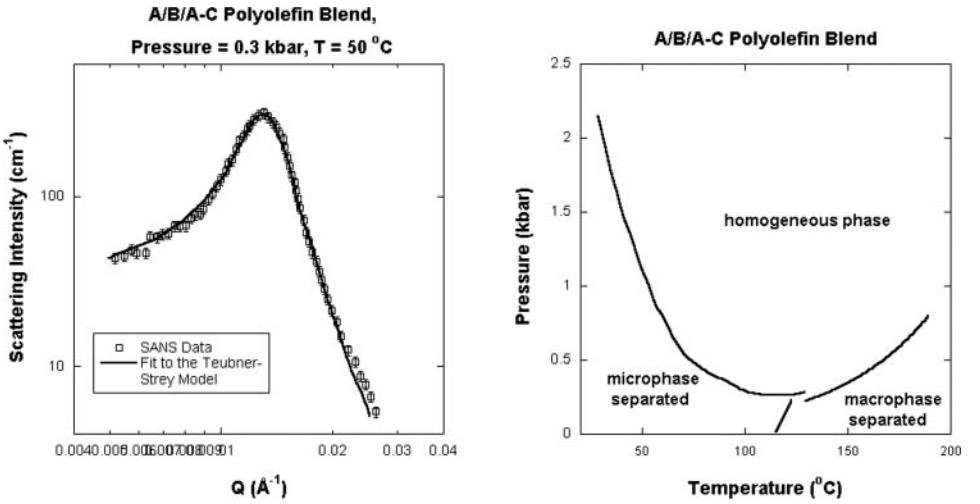

Figure 6. SANS data from A/B/A-C polyolefin blend mixture of two homopolymers A/B and a diblock copolymer A-C under pressure (0.3 kbar) and for a sample temperature of 50 °C (left) and pressure-temperature phase diagram (right). The Teubner-Strey model yields good model fit to the SANS data in the bicontinuous (microphase separated) phase region. The error bars correspond to one standard deviation.

SANS studies were performed to assess the possibility of swelling for high molecular weight "tracer" polymers (poly(ethylene oxide) and poly(methyl methacrylate) in low molecular weight polymer matrix.[23] The same polymers (PEO and PMMA) were used for the matrix component. Three matrices were considered—pure PEO, pure PMMA, and 50%/50% (mass fractions) PEO/PMMA blend. Deuterated polymers were used for the tracer polymers and hydrogenated polymers were used for the matrix polymers. Low tracer polymer fractions were used. Measurement temperatures were chosen to be above the crystal meting temperature of PEO and above the glass-rubber transition temperature of PMMA. The SANS intensity was fit to a Debye function (form factor for unperturbed coils) in order to extract a radius of gyration in each case. The tracer polymers were found to follow unperturbed coil configurations in all cases; no chain swelling was observed.

7. Branched or Grafted Polymers

Many investigations on SANS from branched or grafted polymers have been reported. These include single generation branching (stars and combs) as well as multi-generation branching (dendrimers and arborescent graft polymers).

Polymer chain architecture plays a role in the mixing behavior of polymer blends. A systematic investigation has been undertaken[24] using a series of branched polystyrene macromolecules (Fig. 7) with either varying number of branch points (and fixed number of chain ends) or varying number of chain ends (and fixed number of branch points). All polystyrene macromolecules were carefully synthesized and characterized. They all correspond to the same molecular weight. Blends were prepared using 50%/50% mixtures of linear deuterated polystyrene and branched (hydrogenated) polystyrenes. SANS data were taken from the two groups of blend samples at various temperatures. Random phase approximation (RPA) equations for blend mixtures of linear and specifically branched

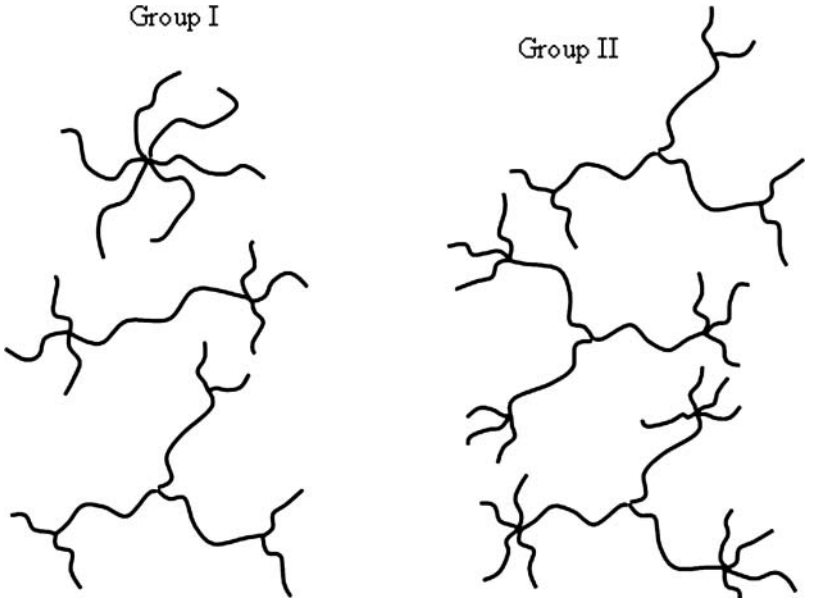

Figure 7. Polymer chain architectures with increasing number of branch points (left) or with increasing number of chain ends (right).

polymers were used to obtain an effective Flory-Huggins interaction parameter χ_{eff} in each case. Partial form factors corresponding to the various regular branching architectures were used as inputs to the RPA fitting approach. The results showed that χ_{eff} increases with increasing number of branch points (group I) and with increasing number of chain ends (group II). Branching seems to favor demixing in polymer blends. A Gaussian field theory was successful in predicting the overall χ_{eff} trend for group II but not for group I.

Arborescent graft polymers containing hyperbranched structures with a polystyrene comb-like backbone and poly(2-vinyl pyridine) chains grafted onto the "teeth" of the comb were investigated in either deuterated water or deuterated methanol dilute solutions.[26] SANS and dynamic light scattering (DLS) were used to characterize the "fast" mode representing the local polyelectrolyte structure and the "slow" mode representing long-range clustering. SANS data showed a polyelectrolyte peak only when the pH was changed by adding hydrochloric acid. This peak is due to the so-called correlation-hole effect and is characteristic of an average distance between charged domains. The peak position scales like polymer fraction to the third power owing to the spherical (3D) symmetry of arborescent polyelectrolytes. Note that for linear polyelectrolytes, the peak position scales like the square root of the polymer fraction (2D symmetry). When enough acid is added to completely neutralize the charges on the P2VP blocks, the polyelectrolyte peak disappears again. Arborescent polymers with longer P2VP grafted blocks resulted in the formation of a gel for fractions greater than 1% mass fraction. The mean spherical approximation model for charged spheres was used to analyze the SANS data when long-range Coulomb interactions are present.

Arborescent polymer sizes and degree of chain swelling were investigated using arborescent polystyrenes with two different size polystyrene side chains (with either 5K or 30K molecular weight) in dilute d-toluene solutions. Generations from G0 to G3 were measured using the SANS technique.[27] A radius of gyration was obtained from the Guinier

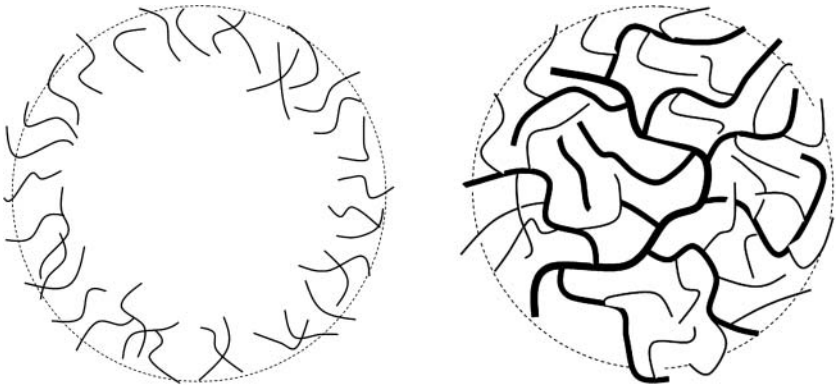

Figure 8. Representation of an arborescent copolymer corresponding to two generations (plus backbone) of h-polystyrene onto which one generation of d-polystyrene was grafted. The h-polystyrene forms the "core" structure whereas the outer d-polystyrene forms the "shell" structure. When the solvent is hydrogenated, only the shell is visible (left) while when the solvent is deuterated, only the core is visible (right).

and the Kratky data analyses methods and compared to the Zimm-Stockmayer model for branched polymer systems with different architectures. This model gives reasonable agreement for the case with short (5 K) side branches but not for the case with long (30 K) side branches. The measured radius of gyration scales with molecular weight for the various generations like $R_g \sim M_w^{0.26}$ for short side branches and $R_g \sim M_w^{0.32}$ for long side branches. Arborescent polymers with long side branches act like compact particles with tight packing. The influence of polymer-solvent interactions on R_g was expressed in terms of the expansion factor due to excluded volume. Swelling effects were clearly observed for short side chains but not for long side chains. Inverse Fourier transforms of the SANS data yielded pair distance distribution functions p(r) which contain information about internal arborescent particle inhomogeneities within the core and within the shell regions. Furthermore, arborescent polymers were synthesized using hydrogenated polystyrene for the core and deuterated polystyrene for the side branches. This helped realize solvent contrast match conditions for either the hydrogenated core or the deuterated shell (Fig. 8) using solvents with more convenient scattering length densities (THF and cyclohexane and their deuterated versions). The higher generation arborescent polymers showed a better-defined core-shell structure than the lower generation ones.

Comblike copolymers with polynorbornene (PNB) backbone and oligo ethylene glycol (OEG) side chains were measured in dilute d-water solutions.[30] The diblock copolymer consists of a (hydrophobic) block with short OEG_3 chains and the other (hydrophilic) block with long $OEG_{6.6}$ chains. SANS measurements were performed over a temperature range between 25°C and 68°C. At 25°C, the copolymers were found to associate into micelles with the hydrophobic block forming an inner spherical core and the hydrophilic block forming cylindrical structures within the outer shell. As the temperature is increased, even long OE $G_{6.6}$ chains become hydrophobic and phase separation occurs at the cloud point temperature of 60°C. Above this temperature, a transition to another phase characterized by sharp Bragg d-spacing of 349 Å is observed. A hybrid model for micelles with spherical core and cylindrical "spokes" radiating out to form the shell was used to analyze the SANS data for low temperatures. A scattering density profile for the micellar shell was obtained

along with an aggregation number. The aggregation number was found to increase and the micellar size was found to decrease with increasing temperature. This is due to the increasing hydrophobicity of OEG chains upon heating.

The hydrophilic block of the previously described diblock copolymer was used to investigate solvent effects in d-toluene and d-water dilute solutions.[31] This corresponds to 50 monomers of norbornene backbone (NB) and oligo ethylene glycol side chains ($OEG_{6.6}$). Four polymer fractions in the dilute solution range and four temperatures between 25°C and 74°C were measured by SANS. Chain dimensions (radius of gyration) and polymer-solvent interactions (second virial coefficient) were obtained from the familiar Zimm plot for dilute polymer solutions. Polymer chains were seen to follow random-coil conformations at low temperature and low polymer fraction when dissolved in d-toluene. Polymers were found to contract with increasing polymer fraction. Deuterated water is a selective solvent for the OEG blocks which tend to take a cylindrical shape forming the teeth of the comblike polymer. The theta temperature was estimated to be 45°C. At 74°C, hydrophobic interactions take over and most of the polymer precipitates out of solution (in d-water).

8. Polymer Gels

Polymer gels form when crosslinking is introduced. The various microstructures formed are in the nanometer length scale making the SANS technique a useful characterization method.

Gels were formed through (electron beam) radiation crosslinking of two diblock copolymers; poly(α-methylstyrene)-polyisoprene (PaMS-PI) and poly(vinylferrocenium triflate)-polyisoprene (PVFT-PI). Radiation crosslinks the PI blocks, induces chain scission in the PaMS blocks, and has no effect on the PVFT blocks. Swelling of the formed gels in partially deuterated solvents allowed the characterization of the crosslink density as function of the radiation dose by SANS, as well as by standard gel characterization methods.[35] This allowed characterization of the copolymer microdomain morphology in the presence of crosslinks. It was found, for instance, that uncrosslinked PaMS blocks play an important role in the swelling behavior of PaMS-PI gels. Chain scission in PaMS seems to release stresses that may appear during gel formation. It was also found that chains in the PVFT blocks undergo stretching as the gel crosslinking becomes tighter. Information about solvent partitioning in the two swollen gels was obtained. Solvent-filled open channels were observed in the PaMS-PI gels whereas large length-scale clustering was observed in PVFT-PI gels.

Poly(vinyl alcohol) hydrogels were formed by introducing physical crosslinks consisting of small ice crystals. These were created through freeze/thaw cycles. Samples that were stretched after the first cycle remained oriented. The PVA hydrogels are intended for potential use in biomedical applications. Their morphology and stress response were investigated using SANS and mechanical testing.[36] Other characterization methods were also used (SAXS, TEM, C-13 NMR, etc.). The Debye-Bueche model was used to obtain a correlation length characterizing the average distance between crosslinks. The Teubner-Strey model was also used to obtain a correlation length along with a quasi-periodic d-pacing characterizing the hydrogel network at the local level. The dominant low-Q feature of the SANS signal was fitted to a power law behavior to represent long-range correlations. SANS results showed that the PVA hydrogel comprises a polymer-rich local phase formed

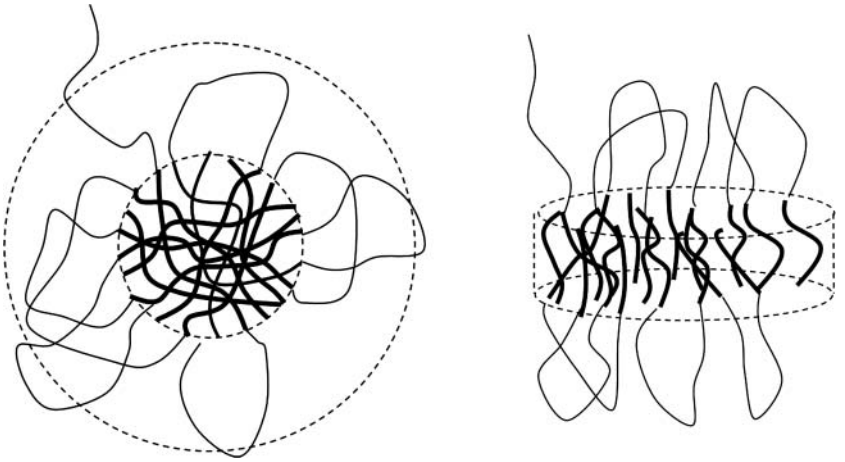

Figure 9. Representation of the flower-like spherical micelle (left) and lamellar micelle (right) formed of triblock copolymers where the central block is hydrophilic and the outer blocks are hydrophobic.

of nanopores 150 to 300 Å in size surrounded by a larger overall structure containing micron size morphology. This structure is held together through the small crystal crosslinks.

PLA-PEO-PLA triblock copolymers are formed of hydrophyllic poly(ethylene oxide) blocks and hydrophobic poly(lactide) blocks. Since the hydrophilic block is the middle block, a flowerlike structure is obtained in water solution (Fig. 9). SANS measurements were made from PLA-PEO-PLA solutions in order to understand the morphology as function of PLA block length and stereospecifity.[38] It was found that spherical micelles form when amorphous D/L-lactic acid blocks are used whereas lamellar micelles form when crystalline L-lactic acid blocks are used. Moreover, an increase in the triblock fraction (in d-water solutions) leads to gel formation. SANS data were analyzed using single micelle form factors and inter-micelle structure factors. In the case of spherical micelles, the familiar Percus-Yevick solution of the Ornsterin-Zernike equation was used while in the case of lamellar micelles, a lamellar stack model introduced to interpret data from lamellar stacks in crystalline polymers in solution was used. Micellar sizes and inter-distances were obtained. The association characteristics of the micelles were found to be controlled by the length and crystallinity of the PLA blocks.

Double-network hydrogels formed of a charged crosslinked polymer network (PAMPS) and neutral linear polyacrylamide (PAA) polymers were investigated using the SANS and Ultra-SANS techniques.[40] The USANS technique can probe size scales up to 20 μm. Deuterated PAA and d-water were used in order to enhance the neutron contrast. Investigation of PAMPS solutions in d-water and of PAMPS/d-PAA solutions in mixtures of d-water and h-water were conducted in order to measure the various Flory-Huggins interaction parameters for the various components. It was found that $\chi_{\text{PAMPS/PAA}} \ll \chi_{\text{PAMS/water}} < \chi_{\text{PAA/water}}$. Measurements from PAMPS/d-PAA/d-water were also taken from the fully formed double-network hydrogels. A random phase approximation model that incorporates charge interactions (through a Debye-Huckel factor) and a crosslinked network (though a characteristic mesh size) was used to fit the SANS data. This model reproduces the high-Q SANS data well and yields some understanding of double-network hydrogel structures at the molecular level.

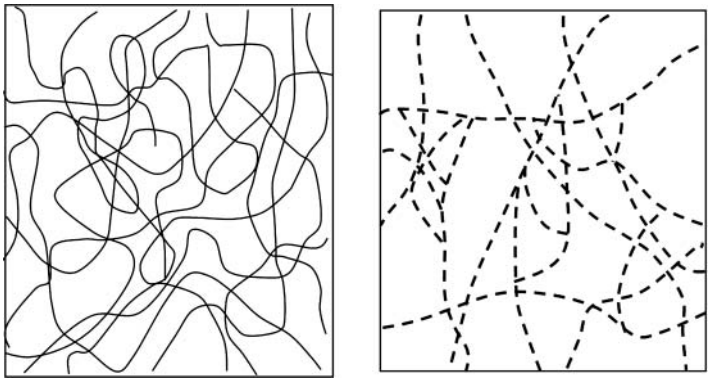

Figure 10. Inhomogeneous structure of PAA (left) and PAMPS (right) polymerized in water as inferred from SANS data.

9. Polymer Networks

The boundary between gels and networks is fuzzy. These appellations could be used interchangeably. Gels usually form beyond a sol-gel transition which is reversible while networks are usually not reversible; they involve covalent crosslinking.

The PAMPS/PAA double-network hydrogel described earlier[40] was used to understand the molecular origin of some unusual mechanical properties (Fig. 10). In-situ SANS investigations were undertaken using samples deformed in a compression device.[41] Molecular conformations of the deuterated PAA chains were monitored. Possible molecular origin of the correlation between enhancement in solution viscosity and fracture toughness of crosslinked gels was discussed. It was argued that molecular association between the PAMPS and PAA components of the double-network could be at the origin of the unusual mechanical performance. The attractive interactions between these two polymers could explain the increased toughness of these polymeric materials.

Polymer blends consisting of stiff liquid crystalline polyurethane and flexible polystyrene-poly(vinyl phenol) copolymers form hydrogen bonded networks characterized by a wide miscibility window.[45] The polystyrene blocks were deuterated to enhance the neutron contrast. SANS measurements from the pure copolymer and with increasing amount of polyurethane allowed the monitoring of crystalline polyurethane chain conformations within an amorphous flexible polymer matrix. FTIR studies showed clear evidence of hydrogen-bonding between the two network components. Increasing the polyurethane fraction succeeded in breaking down the network of hydrogen bonds and led to the formation of new large-scale structures. The semiflexible polyurethane chains assume anisotropic conformations as observed by the SANS high-Q data and fits to the Kratky-Porod wormlike chain model.

Interpenetrating polymer networks (IPNs) are formed through the in-situ synthesis of a network within the matrix of another. The state of miscibility of the mixed components during synthesis dictates the resulting network morphology. SANS and dynamic mechanical thermal analysis (DMTA) were performed on a series of methacrylate/epoxy interpenetrating polymer networks in order to assess the extent of molecular miscibility.[46] SANS is sensitive to composition fluctuations and DMTA can measure the glass-rubber transition temperatures (T_gs) for polymeric materials precisely. A single T_g is a signature of a homogeneously mixed phase while two T_gs point to a demixed two-phase system. The

Debye-Bueche model was used to interpret SANS data from the interpenetrating polymer networks and yielded a phase separation size scale of order 180 Å. DMTA of the rubbery region of some of the IPNs revealed bicontinuous structures and the extent of phase separation.

A number of amphiphilic co-networks of methacrylic acid (MAA) and 2-butyl-1-octyl methacrylate (BOMA) were synthesized and characterized using a host of methods.[48] Some were model co-networks containing A-B-A copolymer chains between cross-links of precise length and composition. Here the A block contains multiple MAA monomers and the B block contains multiple BOMA monomers. The linear co-network precursors used in the group transfer polymerization were characterized by GPC and NMR for their molecular weight and composition. The degree of swelling of these amphiphilic polymer co-networks was investigated in water and in THF over a broad ionization range of the MAA monomers. It was found that the degree of swelling in water increased with the degree of ionization and the size of the MAA blocks. The degree of swelling in THF also increased with the length of the copolymers between cross-link points. The SANS technique and atomic force microscopy were used to characterize the co-network morphology.

10. Polymer Micelles

Water-soluble polymers can form nonionic micelles owing to their hydrophobic/hydrophilic characteristics. Here also, the SANS technique has been an effective tool for the characterization of structure and miscibility.

Wormlike micelles are formed using trimethylammonium cations and 4-vinylbenzoate counterions in aqueous solution. The resulting polymer-surfactant aggregates were polymerized to obtain rodlike ionic micelles.[49] The micelle radius was controlled by varying the hydrocarbon length on the trimethylammonium and its length was controlled by varying the initiator decomposition half-life. This was done by varying temperature or using different initiators. The micelle radius was varied between 17 Å and 24 Å and its length was varied between 800 Å and 5000 Å as characterized by SANS measurements. This approach yielded stable polymerized rodlike micelles with controllable sizes that are independent of surfactant concentration (provided that it is higher than the critical micelle concentration). Long polymerized micelles were obtained using low initiator content and low temperature.

Free radical polymerization of the mixture of cetyltrimethylammonium (CTVB) and sodium 4-styrenesulfonate (NaSS) in aqueous solution produced stable rodlike particles (Fig. 11) with controlled surface charge density.[51] Rodlike particle dimensions were

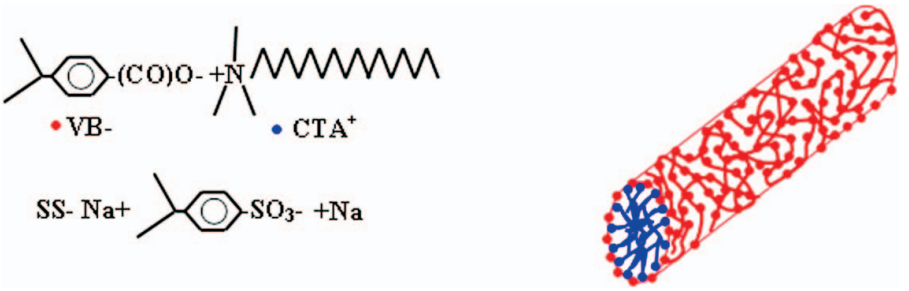

Figure 11. Chemical representation of CTVB and NaSS (left) and schematic representation of the polymerized rodlike micelle (right).

characterized by SANS; the diameter was found to be constant (equal to 40 Å) and the length varied between 240 Å and 850 Å depending on NaSS concentration. When the NaSS concentration was increased, the rodlike particle length increased then decreased. The longest particles were obtained at the charge neutralization condition. Zeta potential measurements were also performed to characterize NaSS charge effects.

Polymer micelles were formed using an A-C diblock copolymer (acting as surfactant) mixed with A and B homopolymers. The C block was characterized by repulsive interactions with the A block but attractive interactions with the B block.[56] This project was also included in earlier sections (SANS from copolymers and blends). The SANS technique was effective at mapping out a microphase separation region, a macrophase separation (two-phase) region, and a homogeneously mixed (one-phase) region in-between. The random phase approximation (RPA), the self-consistent-field theory (SCFT) and Teubner-Strey (TS) model were used to analyze the SANS data. Reasonable agreements were found.

Small molecule surfactants cause the melting of polymeric micelles formed of amphiphilic diblock copolymers. The poly(butylacrylate)-poly(acrylic acid) (PBA-PAA) diblock forms micelles in aqueous solution. Neutral or ionic surfactants (such as C12E6 for example) break the polymer micelles as documented by light scattering (SLS and DLS), SAXS, SANS, cryo-TEM, and capillary electrophoresis;[58] they reduce the interfacial tension and gradually produce two populations—one rich in large polymer micelles and one rich in small surfactant micelles. Before adding small surfactants, fits of a core-shell model to SANS data yielded an estimate of the core radius for the polymeric micelles around 80 Å (polydispersity of 0.2). After adding 1.5% mass fraction of C12E6 small molecule surfactant, the mean micelle radius decreased to 34 Å (polydispersity of 0.14). This size (34 Å) is very close to the size of pure-surfactant micelles. Simple interfacial tension arguments with and without surfactant permits the interpretation of the observed trends.

A model hydrophobically modified polymer was used to crosslink wormlike micelles[59] in water. Water-soluble poly(ethylene oxide) containing hydrocarbon tails (C_{14} to C_{22}) at their ends was used to form bridges across wormlike micelles (1% mass fraction CTAT in water). SANS and rheology were used to characterize crosslinked network. The hydrophobic end groups stick to the wormlike micelles while PEO chains remain dissolved. Three types of PEO chains were used—

1. PEO chains with a sticker at one end, 2. PEO chains with a sticker at each end, and 3. 3-arm PEO stars with a sticker at each end.

The wormlike micelles are likely breaking locally and reforming to shield the hydrophobic stickers from contact with water. The PEO chains form bridges between the wormlike micelles (Fig. 12).

Pluronic triblock copolymers (PEO-PPO-PEO) form micellar structures at ambient temperatures. Spherical micelles formed when Pluronic F127 solutions in d-water (20% mass fraction) were sheared in a Couette shear cell. In-situ SANS investigations were performed using the radial and tangential neutron beam configurations.[60] The spherical micelles were seen to form layered macrolattice structures characterized by single-crystal type scattering (with bright diffraction spots). Transition from face-centered cubic structure at low shear rates to random layer stacking at high shear rates was observed. This was the cause of the observed shear thinning behavior. A model comprising intra-layer sphere arrangement as well as inter-layer structure was used to interpret the SANS data under shear. This model incorporated oriented stacks of micellar layers and allowed for disorder

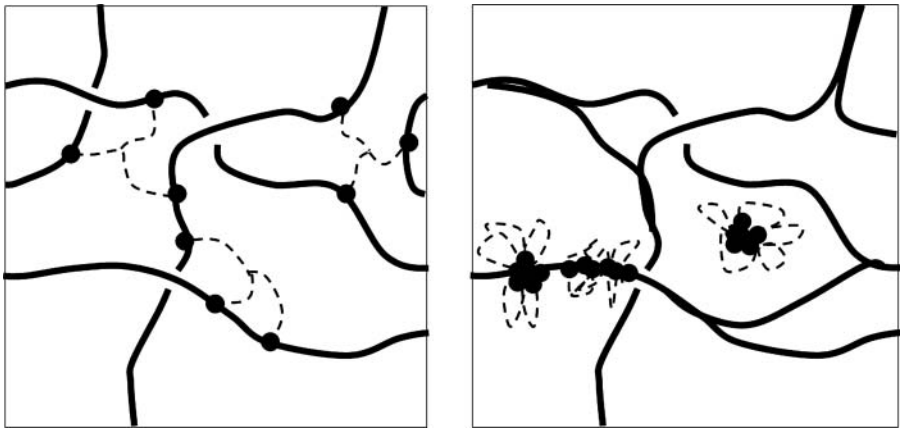

Figure 12. Two possible clustering configurations. There is evidence that the configuration on the left is more likely than the one on the right.

effects; it reproduced the observed cubic structures and a transition to random layer stacking leading to a hexagonal phase.

The SANS technique was used to investigate the structure of polystyrene-poly(acrylic acid, sodium salt) copolymers in water solution under Couette and plate-plate shear.[63] This investigation reported a wide range of copolymer fractions in water solution using PS-PAA of $M_n = 4{,}700$–$11{,}300$ g/mol. Since the polystyrene block is hydrophobic, wormlike micelles form. These were found to form hexagonally close-packed cylinders under shear with the cylinder axis parallel to the shear gradient direction; i.e., perpendicular to the shear flow direction. SAXS and electron microcopy confirmed the oriented cylinders structure. Evidence for bridging between cylinders was reported. This may be due to the long PAA block length and some clustering driving force which depends on the cylindrical micelle fraction.

11. Polymeric Nanomaterials

This is a category gathering SANS investigations from various materials including those described here.

SANS from mixtures of deuterated and non-deuterated isotopic blends is a good monitor of chain orientation in (for instance) injection-molded samples. A series of isotopic polystyrene blends has been injection molded, while varying a number of experimental conditions, including injection molding speed, mold thickness, and mold temperature.[64] Elliptical averaging of the anisotropic 2D data yielded an eccentricity factor which is a measure of the degree of chain orientation. This eccentricity factor was found to decrease with injection speed, mold thickness, and injection molding temperature. It was also found to decrease with the length scale probed showing that nano-stresses acting upon polymer chains relax at the local chain segment level.

SANS and x-ray reflectometry have been used to characterize the porosity of a poly(phenylene) low-k dielectric thin film material.[65] This material contains porogen which degrades upon baking at elevated temperatures thereby forming the pores. Three baking temperatures were used (150°C, 400°C, and 430°C). Since the thickness of each film was around 1 micron, many wafers were stacked in order to enhance the SANS signal. The

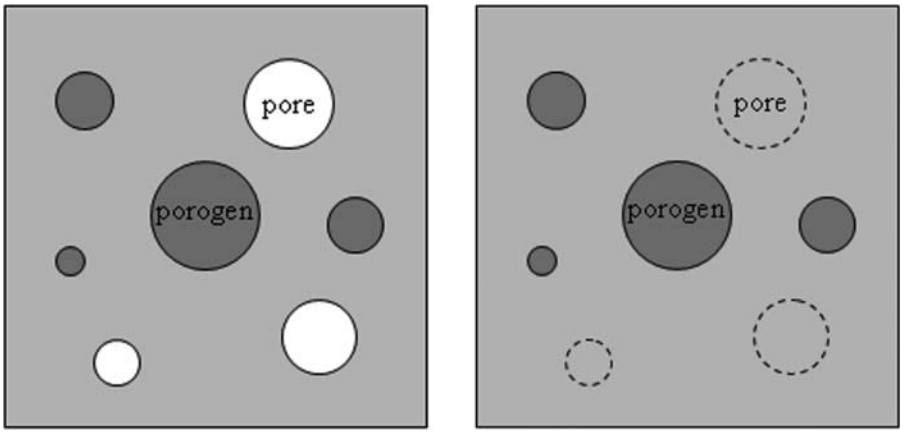

Figure 13. Porosity representation of the low-k dielectric material containing porogen after baking at 400°C without (left) and with solvent contrast match (right). The partially deuterated solvent vapor matches the scattering length density of the matrix and fills the pores making them invisible.

samples were placed in a custom-built flow-through cell in order to control the vapor pressure. Mixtures of deuterated and non-deuterated methanol or toluene solvent vapors were used to adjust the neutron contrast by filling the pores (Fig. 13). The pore size distribution and pore fraction were determined for each baking strategy. The fraction of porogen that remains in the low-k films was estimated and found to decrease with baking temperature.

Body armors are made out of high strength material containing poly(p-phenylene-2,6-benzobisoxazole) fibers. An extensive study of such material aged at elevated temperatures for extended periods of time (around half a year) was conducted using a battery of characterization methods including mechanical testing (tensile strength measurements), SANS, FTIR, atomic force microscopy, and confocal microscopy.[66] A 30% decrease in yarn tensile strength upon aging in humid environment was correlated with the hydrolysis of specific chemical groups as observed by FTIR. When aging was performed in an inert (argon) environment, this decrease went down to 4%. This demonstrates that moisture is a key factor in fiber degradation.

SANS studies were conducted on composites formed of isotopic polystyrene blends mixed with silica nanoparticles under contrast match condition.[69] It was found that polymer chain conformations follow unperturbed Gaussian chain statistics regardless of polymer molecular weight and nanoparticle loading. The polymer reference interaction site model (RISM) was used to model polymer/nanoparticle interactions.

12. Polymer Membranes

The hydrogen fuel cell technology has become an active SANS area of research. Fuel cells use hydrogen to produce electricity. Hydrogen fuel is channeled to the anode on one side while oxygen is channeled to the cathode on the other side. At the anode, a catalyst causes hydrogen to ionize into protons and electrons. The polymer membrane allows only the protons to pass through to the cathode. The electrons, on the other hand, travel along an external circuit thereby generating an electrical current (Fig. 14). SANS has been used to characterize the structure of some polymer membranes.

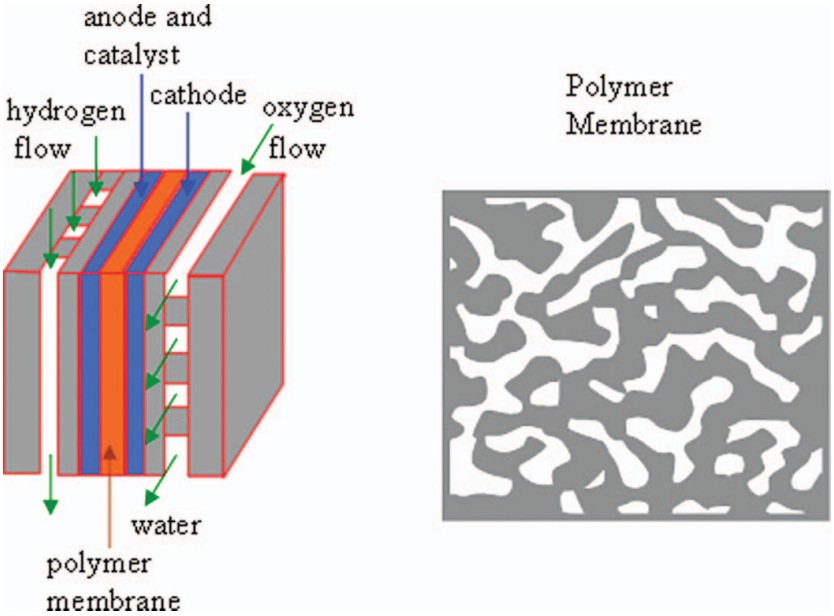

Figure 14. Schematics of a hydrogen fuel cell (left) and bicontinuous morphology of a polymer membrane (right).

Poly(perfluorosulfonic acid) also referred to as Nafion is a fuel cell membrane material. SANS investigations have been conducted on Nafion membranes in an in-situ vapor sorption cell used to control the relative humidity.[71] Different membrane processing conditions (melt extrusion or solvent casting), thermal pretreatment histories, and submicron membrane thicknesses were studied. The SANS data showed features characterizing semicrystalline copolymers and porous media with ion channels in the nanometer size range. A strong correlation was found between the interionic domain distance and the relative humidity. Diffusion coefficients of water vapor were estimated based on the observed structural evolution.

Diblock copolymer films composed of a fluorocarbon block and a sulfonated polystyrene block were investigated by SANS and TEM.[73] These are the potential proton exchange membranes for low-temperature fuel cells. Two hierarchical structure levels were observed—one due to the block copolymer microstructure and one due to the charged domains structure. The copolymer microstructure shows clearly fluorous domains and sulfonated polystyrene (darker) domains by TEM. Longer and partially sulfonated polystyrene blocks yield well-ordered microdomains, whereas shorter and fully sulfonated polystyrene blocks yield more disordered structures.

Polystyrene sulfonate-b-poly(methyl butytlene) block copolymers have also been investigated as potential membrane material for hydrogen fuel cells.[75] The microdomain morphology was controlled by varying the molecular weight of the polystyrene sulfonate (PSS) block and therefore the size of the hydrophilic proton channels. A drastic trend reversal was observed for channel sizes around 50 Å. The proton conductivity was found to decrease with increasing temperature for channel sizes higher than 50 Å (i.e., when high molecular weight PSS blocks are used) and to increase with increasing temperature for channel sizes smaller than 50 Å (i.e., when low molecular weight PSS blocks are used).

These findings were supported from evidence based on TEM and SANS studies. Some of these studies were conducted under systematic moisture control. The correlation between the moisture content and proton conductivity in these membranes was clearly demonstrated.

The phase behavior of one of the above-described block copolymer PSS-PMB used as ion-containing membrane has been investigated as function of relative humidity (RH). The copolymer ion content (sulfonation level) represented by the ion-exchange capacity (IEC) parameter was varied as well as the membrane temperature.[76] SAXS, TEM, SANS, DSC and water content measurements were used to probe the rich phase behavior. Indexing of the various SAXS Bragg peaks helps in structure determination. The disordered phase was observed for low IEC and low RH values, the gyroid phase was observed for high IEC and low RH values, whereas the lamellar phase was observed for high RH values.

13. Summary and Future Prospect

Use of the SANS technique has been ever-growing in the area of polymer research. Improvements of SANS instrument capabilities, sophistication of data analysis methods, and the advent of judicious sample environments have brought about renewed interest over the past thirty years. One of the leading SANS research centers, the NCNR, operates two 30 m SANS instruments in the user mode. This attracts over 200 SANS users per year resulting in over 80 publications in refereed journals. Polymer research constitute about one-third of this effort.

Increased demand for additional SANS beamtime is the driving force behind a major upgrade of the NCNR facility. This upgrade includes the construction of a higher resolution SANS instrument. The new 40 m VSANS instrument (V is for "very") will lower the measurement range (Q_{min}) by an order of magnitude without too much loss in neutron flux on sample. The new (lower) Q_{min} will be around 0.0002 $Å^{-1}$ which will be achieved by using multiple-hole converging collimation. The measurement window of the VSANS instrument will overlap nicely with the Bonse-Hart USANS instrument. The new capability VSANS/USANS combination will cover 5 orders of magnitude in scattering variable. This will allow the probing of polymer structures from the near atomic (nanometer) scale to well into the optical (20 micrometers) size scale and will open up exciting new prospects for polymer research. Other neutron scattering facilities in the US, in Europe, as well as elsewhere are also thriving. The SANS technique is the major driving force fueling the success of these facilities.

Disclaimer/Acknowledegments

Certain commercial equipment, instruments, or materials are identified in this paper to foster understanding. Such identification does not imply recommendation or endorsement by the National Institute of Standards and Technology, nor does it imply that the materials or equipments identified are necessarily the best available for the purpose. This work is based upon activities supported in part by the National Science Foundation under Agreement No. DMR-0454672.

References

1. Hammouda, B. Probing nanoscale structures—The SANS toolbox, 2009, available online at http:www.ncnr.nist.gov/staff/hammouda/the_sans_toolbox.pdf.

2. Yun, S. I.; Terao, K.; Hong, K.; Melnichenko, Y. B.; Wignall, G. D.; Britt, P. F.; Mays, J. W. "Solution properties of 1,3-cyclohexadiene polymers by laser light scattering and small-angle neutron scattering," *Macromolecules,* **2006**, *39*, 897–899.
3. Hammouda, B. "Solvation characteristics of a model water-soluble polymer," *Journal of Polymer Science: Part B: Polymer Physics*, **2006**, *44*, 3195–3199.
4. Hammouda, B., Ho, D. L. "Insight into chain dimensions in PEO/water solutions," *Journal of Polymer Science: Part B: Polymer Physics,* **2007**, *45*, 2196–2200.
5. Norman, A. I.; Fei, Y.; Ho, D. L.; Greer, S. C. "Folding and unfolding of polymer helices in solution," *Macromolecules,* **2007**, *40*, 2559–2567.
6. Norman, A. I.; Ho, D. L.; Greer, S. C. "Partitioning, fractionation, and conformations of star poly(ethylene glycol) in isobutyric acid and water," *Macromolecules,* **2007**, *40*, 9628–9639.
7. Rahman, M. H.; Chen, C. Y.; Liao, S. C.; Chen, H. L.; Tsao, C. S.; Chen, J. H.; Liao, J. L.; Ivanov, V. A.; Chen, S. A. "Segmental alignment in the aggregate domains of poly(9,9-dioctylfluorene) in semidilute solution," *Macromolecules,* **2007**, *40*, 6572–6578.
8. Wang, H. "SANS study of the early stages of crystallization in polyethylene solutions," *Polymer,* **2006**, *47*, 4897–4900.
9. Ho, D. L.; Hammouda, B.; Kline, S. R.; Chen, W. R. "Unusual phase behavior in mixtures of poly(ethylene oxide) and ethyl Alcohol," *Journal of Polymer Science: Part B: Polymer Physics*, **2006**, *44*, 557–564.
10. Wu, L.; Lodge, T. P.; Bates, F. S. "SANS determination of chain conformation in perpendicular-aligned undecablock copolymer lamellae," *Macromolecules,* **2006**, *39*, 294–299.
11. Foster, L. J. R.; Knott, R.; Sanguanchaipaiwong, V.; Holden, P. J. "Polyhydroxyalkanoate-based natural–synthetic hybrid copolymer films: A small-angle neutron scattering study," *Physica B,* **2006**, *385–386*, 770–772.
12. Norman, A. I.; Ho, D. L.; Lee, J. H.; Karim, A. "Spontaneous formation of vesicles of diblock copolymer EO6BO11 in water: A SANS study," *J. Phys. Chem. B,* **2006**, *110*, 62–67.
13. Triftaridou, A. I.; Vamvakaki, M.; Patrickios, C. S. "Cationic amphiphilic model networks based on symmetrical ABCBA pentablock terpolymers: Synthesis, characterization, and modeling," *Biomacromolecules,* **2007**, *8*, 1615–1623.
14. Jacquin, M.; Muller, P.; Talingting-Pabalan, R.; Cottet, H.; Berret, J. F.; Futterer, T.; Théodoly, O. "Chemical analysis and aqueous solution properties of charged amphiphilic block copolymers PBA-*b*-PAA synthesized by MADIX," *Journal of Colloid and Interface Science,* **2007**, *316*, 897–911.
15. Agrawal, S. K.; Sanabria-DeLong, N.; Jemian, P. R.; Tew, G. N.; Bhatia, S. R. "Micro- to nanoscale structure of biocompatible PLA-PEO-PLA hydrogels," *Langmuir,* **2007**, *23*, 5039–5044.
16. Francis, T. J.; Vogt, B. D.; Wang, M. X.; Watkins, J. J. "Scaling of interdomain spacing of diblock copolymers in a selective diluent," *Macromolecules,* **2007**, *40*, 2515–2519.
17. Park, M. J.; Balsara, N. P. "Phase behavior of symmetric sulfonated block copolymers," *Macromolecules,* **2008**, *41*, 3678–3687.
18. Zhou, N.; Lodge, T. P.; Bates, F. S. "Influence of conformational asymmetry on the phase behavior of ternary homopolymer/block copolymer blends around the bicontinuous microemulsion channel," *J. Phys. Chem. B,* **2006**, *110*, 3979–3989.
19. Ruegg, M. L.; Reynolds, B. J.; Lin, M. Y.; Lohse, D. J.; Balsara, N. P. "Minimizing the concentration of diblock copolymer needed to organize blends of weakly segregated polymers by tuning attractive and repulsive interactions," *Macromolecules,* **2007**, *40*, 1207–1217.
20. Ruegg, M. L.; Reynolds, B. J.; Lin, M. Y.; Lohse, D. J.; Krishnamoorti, R., Balsara, N. P. "Effect of pressure on a multicomponent A/B/A-C polymer blend with attractive and repulsive interactions," *Macromolecules,* **2007**, *40*, 355–365.
21. Patel, A. J.; Balsara, N. P. "Observing nucleation close to the binodal by perturbing metastable polymer blends," *Macromolecules,* **2007**, *40*, 1675–1683.
22. Wanakule, N. S.; Nedoma, A. J.; Robertson, M. L.; Fang, X.; Jackson, A.; Garetz, B. A.; Balsara, N. P. "Characterization of micron-sized periodic structures in multicomponent polymer blends

by ultra-small-angle neutron scattering and optical microscopy," *Macromolecules,* **2008**, *41*, 471–477.
23. Zeroni, I.; Lodge, T. P. "Chain dimensions in poly(ethylene oxide)/poly(methyl methacrylate) blends," *Macromolecules,* **2008**, *41*, 1050–1052.
24. Lee, J. S.; Foster, M. D.; Wu, D. T. "Effects of branch points and chain ends on the thermodynamic interaction parameter in binary blends of regularly branched and linear polymers," *Macromolecules,* **2006**, *39*, 5113–5121.
25. Rathgeber, S.; Monkenbusch, M.; Hedrick, J. L.; Trollsas, M.; Gast, A. P. "Starlike dendrimers in solutions: Structural properties and internal dynamics," *The Journal of Chemical Physics,* **2006**, *125*, 204908-1 to 204908-11.
26. Yun, S. I.; Briber, R. M.; Kee, R. A.; Gauthier, M. "Dilute-solution structure of charged arborescent graft polymer," *Polymer,* **2006**, *47*, 2750–2759.
27. Yun, S. I.; Lai, K. C.; Briber, R. M.; Teertstra, S. J.; Gauthier, M.; Bauer, B. J. "Conformation of arborescent polymers in solution by small-angle neutron scattering: Segment density and core-shell morphology," *Macromolecules,* **2008**, *41*, 175–183.
28. Chen, W. R.; Porcar, L.; Liu, Y.; Butler, P. D.; Magid, L. J. "Small angle neutron scattering studies of the counterion effects on the molecular conformation and structure of charged G4 PAMAM dendrimers in aqueous solutions," *Macromolecules,* **2007**, *40*, 5887–5898.
29. Cheng, G.; Melnichenko, Y. B.; Wignall, G. D.; Hua, F.; Hong, K.; Mays, J. W. "Conformation of oligo(ethylene glycol) grafted polystyrene in dilute aqueous solutions," *Polymer,* **2007**, *48*, 4108–4113.
30. Cheng, G.; Hua, F.; Melnichenko, Y. B.; Hong, K.; Mays, J. W.; Hammouda, B.; Wignall, G. D. "Association and structure of thermosensitive comblike block copolymers in aqueous solutions," *Macromolecules,* **2008**, *41*, 4824–4827.
31. Cheng, G.; Hua, F.; Melnichenko, Y. B.; Hong, K.; Mays, J. W.; Hammouda, B.; Wignall, G. D. "Conformation of oligo(ethylene glycol) grafted poly(norbornene) in solutions: A small angle neutron scattering study" *European Polymer Journal,* **2008**, *44*, 2859–2864.
32. Mortensen, K.; Gasser, U.; Gursel, S. A.; Scherer, G. G. "Structural characterization of radiation-grafted block copolymer films using SANS technique," *Journal of Polymer Science: Part B: Polymer Physics*, **2008**, *46*, 1660–1668.
33. Loizou, E.; Butler, P.; Porcar, L.; Schmidt, G. "Dynamic responses in nanocomposite hydrogels," *Macromolecules,* **2006**, *39*, 1614–1619.
34. Matos, M. A.; White, L. R.; Tilton, R. D. "Electroosmotically enhanced mass transfer through polyacrylamide gels," *Journal of Colloid and Interface Science,* **2006**, *300*, 429–436.
35. Durkee, D. A.; Gomez, E. D.; Ellsworth, M. W.; Bell, A. T.; Balsara, N. P. "Microstructure and solvent distribution in cross-linked diblock copolymer gels," *Macromolecules,* **2007**, *40*, 5103–5110.
36. Millon, L. E.; Nieh, M. P.; Hutter, J. L.; Wan, W. "SANS characterization of an anisotropic poly(vinyl alcohol) hydrogel with vascular applications," *Macromolecules,* **2007**, *40*, 3655–3662.
37. Jiang, J.; Malal, R.; Li, C.; Lin, M. Y.; Colby, R. H.; Gersappe, D.; Rafailovich, M. H.; Sokolov, J. C.; Cohn, D. "Rheology of thermoreversible hydrogels from multiblock associating copolymers," *Macromolecules,* **2008**, *41*, 3646–3652.
38. Agrawal, S. K.; Sanabria-DeLong, N.; Tew, G. N.; Bhatia, S. R. "Structural characterization of PLA-PEO-PLA solutions and hydrogels: Crystalline vs amorphous PLA domains," *Macromolecules,* **2008**, *41*, 1774–1784.
39. Tirumala, V. R.; Tominaga, T.; Lee, S.; Butler, P. D.; Lin, E. K.; Gong, J. P.; Wu, W. L. "Molecular model for toughening in double-network hydrogels," *J. Phys. Chem. B,* **2008**, *112*, 8024–8031.
40. Tominaga, T.; Tirumala, V. R.; Lee, S.; Lin, E. K.; Gong, J. P.; Wu, W. L. "Thermodynamic interactions in double-network hydrogels," *J. Phys. Chem. B,* **2008**, *112*, 3903–3909.
41. Tominaga, T.; Tirumala, V. R.; Lin, E. K.; Gong, J. P.; Furukawa, H.; Osada, Y.; Wu, W. L. "The molecular origin of enhanced toughness in doublenetwork hydrogels: A neutron scattering study," *Polymer,* **2007**, *48*, 7449–7454.

42. Sun, Y. S.; Jeng, U. S.; Huang, Y. S.; Liang, K. S.; Lin, T. L.; Tsao, C. S. "Complementary SAXS and SANS for structural characteristics of a polyurethethane elastomer of low hard-segment content," *Physica B,* **2006**, *385–386*, 650–652.
43. Li, Y. C.; Chen, K. B.; Chen, H. L.; Hsu, C. S.; Tsao, C. S.; Chen, J. H.; Chen, S. A. "Fractal aggregates of conjugated polymer in solution state," *Langmuir,* **2006**, *22*, 11009–11015.
44. Burford, R. P.; Markotsis, M. G.; Knott, R. B. "Real-time SANS study of interpenetrating polymer network (IPN) formation," *Physica B,* **2006**, *385–386*, 766–769.
45. Mehta, R.; Dadmun, M. D. "Small angle neutron scattering studies on miscible blends of poly(styrene-*ran*-vinyl phenol) with liquid crystalline polyurethane," *Macromolecules,* **2006**, *39*, 8799–8807.
46. Dean, K. M.; Cook, W. D.; Lin, M. Y. "Small angle neutron scattering and dynamic mechanical thermal analysis of dimethacrylate/epoxy IPNs," *European Polymer Journal,* **2006**, *42*, 2872–2887.
47. Kali, G.; Georgiou, T. K.; Ivan, B.; Patrickios, C. S.; Loizou, E.; Thomann, Y.; Tiller, J. C. "Synthesis and characterization of anionic amphiphilic model co-networks based on methacrylic acid and methyl methacrylate: Effects of composition and architecture," *Macromolecules,* **2007**, *40*, 2192–2200.
48. Kali, G.; Georgiou, T. K.; Iván, B.; Patrickios, C. S.; Loizou, E.; Thomann, Y.; Tiller, J. C. "Synthesis and characterization of anionic amphiphilic model co-networks of 2-Butyl-1-octyl-methacrylate and methacrylic acid: Effects of polymer composition and architecture," *Langmuir,* **2007**, *23*, 10746–10755.
49. Gerber, M. J.; Walker, L. M. "Controlling dimensions of polymerized micelles: Micelle template versus reaction conditions," *Langmuir,* **2006**, *22*, 941–948.
50. Kuntz, D. M.; Walker, L. M. "Solution behavior of rod-like polyelectrolyte-surfactant aggregates polymerized from wormlike micelles," *J. Phys. Chem. B,* **2007**, *111*, 6417–6424.
51. Kim, T. H.; Choi, S. M.; Kline, S. R. "Polymerized rodlike nanoparticles with controlled surface charge density," *Langmuir,* **2006**, *22*, 2844–2850.
52. Kim, T. H.; Doe, C.; Kline, S. R.; Choi, S. M. "Water redispersible isolated single-walled carbon nanotubes fabricated by in-situ polymerization of micelles," *Adv. Mater*. **2007**, *19*, 929–933.
53. Pozzo, D. C.; Walker, L. M. "Shear orientation of nanoparticle arrays templated in a thermoreversible block copolymer micellar crystal," *Macromolecules,* **2007**, *40*, 5801–5811.
54. Pozzo, D. C.; Walker, L. M. "Small-angle neutron scattering of silica nanoparticles templated in PEO–PPO–PEO cubic crystals" *Colloids and Surfaces A: Physicochem. Eng. Aspects,* **2007**, *294*, 117–129.
55. Pozzo, D. C.; Walker, L. M. "Macroscopic alignment of nanoparticle arrays in soft crystals of cubic and cylindrical polymer micelles," *Eur. Phys. J. E,* **2008**, *26*, 183–189.
56. Ruegg, M .L.; Reynolds, B. J.; Lin, M. Y.; Lohse, D. J.; Balsara, N. P. "Microphase and macrophase separation in multicomponent A/B/A-C polymer blends with attractive and repulsive interactions," *Macromolecules,* **2006**, *39*, 1125–1134.
57. Gomez, E. D.; Ruegg, M. L.; Minor, A. M.; Kisielowski, C.; Downing, K. H.; Glaeser, R. M.; Balsara, N. P. "Interfacial concentration profiles of rubbery polyolefin lamellae determined by quantitative electron microscopy," *Macromolecules,* **2008**, *41*, 156–162.
58. Jacquin, M.; Muller, P.; Cottet, H.; Crooks, R.; Thé odoly, O. "Controlling the melting of kinetically frozen poly(butylacrylate-*b*-acrylic acid) micelles via addition of surfactant," *Langmuir,* **2007**, *23*, 9939–9948.
59. Lodge, T. P.; Taribagil, R.; Yoshida, T.; Hillmyer, M. A. "SANS evidence for the cross-linking of wormlike micelles by a model hydrophobically modified polymer," *Macromolecules,* **2007**, *40*, 4728–4731.
60. Jiang, J.; Burger, C.; Li, C.; Li, J.; Lin, M. Y.; Colby, R. H.; Rafailovich, M. H.; Sokolov, J. C. "Shear-induced layered structure of polymeric micelles by SANS," *Macromolecules,* **2007**, *40*, 4016–4022.

61. Jiang, J.; Li, C.; Lombardi, J.; Colby, R. H.; Rigas, B.; Rafailovich, M. H.; Sokolov, J. C. "The effect of physiologically relevant additives on the rheological properties of concentrated Pluronic copolymer gels," *Polymer,* **2008**, *49*, 3561–3567.
62. O'Driscoll, B. M. D.; Hawley, A. M.; Edler, K. J. "Incorporation of sparingly soluble species in mesostructured surfactant–polymer films," *Journal of Colloid and Interface Science,* **2008**, *317*, 585–592.
63. Grandjean, J.; Mourchid, A. "Restricted swelling and its orientation effect on copolymer micellar solutions of hexagonal-packed cylinders under steady shear flow," *Langmuir,* **2008**, *24*, 2318–2325.
64. Healy, J.; Edward, G. H.; Knott, R. B. "Residual orientation in injection micro-molded samples," *Physica B,* **2006**, *385–386*, 620–622.
65. Silverstein, M. S.; Bauer, B. J.; Hedden, R. C.; Lee, H. J.; Landes, B. G. "SANS and XRR porosimetry of a polyphenylene low-k dielectric," *Macromolecules,* **2006**, *39*, 2998–3006.
66. Chin, J.; Forster, A.; Clerici, C.; Sung, L.; Oudina, M.; Rice, K. "Temperature and humidity aging of poly(p-phenylene-2,6- benzobisoxazole) fibers: Chemical and physical characterization," *Polymer Degradation and Stability,* **2007**, *92*, 1234–1246.
67. Stefanescu, E. A.; Dundigalla, A.; Ferreiro, V.; Loizou, E.; Porcar, L.; Negulescu, I.; Garno, J.; Schmidt, G. "Supramolecular structures in nanocomposite multilayered films," *Phys. Chem. Chem. Phys.,* **2006**, *8*, 1739–1746.
68. Li, J.; Jiang, J.; Li, C.; Lin, M. Y.; Schwarz, S. A.; Rafailovich, M. H.; Sokolov, J. "Effect of temperature on shear-induced anisotropic structure in polymer clay hydrogels," *Macromol. Rapid Commun*. **2006**, *27*, 1787–1791.
69. Sen, S.; Xie, Y.; Kumar, S. K.; Yang, H.; Bansal, A.; Ho, D. L.; Hall, L.; Hooper, J. B.; Schweizer, K. S. "Chain conformations and bound-layer correlations in polymer nanocomposites," *Phys. Rev. Lett.,* **2007**, *98*, 128302-1 to 128302-4.
70. Chatterjee, T.; Krishnamoorti, R. "Dynamic consequences of the fractal network of nanotube-poly(ethylene oxide) nanocomposites," *Physical Review E,* **2007**, *75*, 050403-1 to 050403-4.
71. Kim, M. H.; Glinka, C. J.; Grot, S. A.; Grot, W. G. "SANS study of the effects of water vapor sorption on the nanoscale structure of perfluorinated sulfonic acid (Nafion) membranes," *Macromolecules,* **2006**, *39*, 4775–4787.
72. Gao, J.; Yang, Y.; Lee, D.; Holdcroft, S.; Frisken, B. J. "Self assembly of latex particles into proton-conductive membranes," *Macromolecules,* **2006**, *39*, 8060–8066.
73. Rubatat, L.; Shi, Z.; Diat, O.; Holdcroft, S.; Frisken, B. J. "Structural study of proton-conducting fluorous block copolymer membranes," *Macromolecules,* **2006**, *39*, 720–730.
74. Shin, K.; Obukhov, S.; Chen, J. T.; Huh, J.; Hwang, Y.; Mok, S.; Dobriyal, P.; Thiyagarajan, P.; Russell, T. P. "Enhanced mobility of confined polymers," *Nature Materials,* **2007**, *6*, 961–965.
75. Park, M. J.; Downing, K. H.; Jackson, A.; Gomez, E. D.; Minor, A. M.; Cookson, D.; Weber, A. Z.; Balsara, N. P. "Increased water retention in polymer electrolyte membranes at elevated temperatures assisted by capillary condensation," *Nano Letters,* **2007**, *7*, 3547–3552.
76. Park, M. J.; Nedoma, A. J.; Geissler, P. L.; Balsara, N. P.; Jackson, A.; Cookson, D. "Humidity-induced phase transitions in ion-containing block copolymer membranes," *Macromolecules,* **2008**, *41*, 2271–2277.
77. Nieh, M. P.; Guiver, M. D.; Kim, D. S.; Ding, J.; Norsten, T. "Morphology of comb-shaped proton exchange membrane copolymers based on a neutron scattering study," *Macromolecules,* **2008**, *41*, 6176–6182.